

Ring polymers in confined geometries

Z. Usatenko¹, J. Halun², P. Kuterba²

¹ Institute of Physics, Cracow University of Technology, 30-084 Cracow, Poland

² Institute of Physics, Jagiellonian University, 30-348 Cracow, Poland

Received June 25, 2016, in final form September 6, 2016

The investigation of a dilute solution of phantom ideal ring polymers and ring polymers with excluded volume interactions (EVI) in a good solvent confined in a slit geometry of two parallel repulsive walls and in a solution of colloidal particles of big size was performed. Taking into account the correspondence between the field theoretical ϕ^4 $O(n)$ -vector model in the limit $n \rightarrow 0$ and the behaviour of long-flexible polymers in a good solvent, the correspondent depletion forces and the forces which exert phantom ideal ring polymers and ring polymers with EVI on the walls were obtained in the framework of the massive field theory approach at fixed space dimensions $d=3$ up to one-loop order. Besides, taking into account the Derjaguin approximation, the depletion forces between big colloidal particle and a wall and in the case of two big colloidal particles were calculated. The obtained results indicate that phantom ideal ring polymers and ring polymers with EVI due to the complexity of chain topology and for entropical reasons demonstrate a completely different behaviour in confined geometries compared with linear polymers.

Key words: *colloidal systems, critical phenomena, polymers, phase transitions*

PACS: *64.70.pv, 61.25.he, 67.30.ej, 68.35.Rh, 64.70.qd*

As it was shown in a series of the atomic force spectroscopy (AFM) experiments [1, 2], biopolymers such as DNA very often present a ring topology. Such a situation takes place, for example, in the case of Escherichia coli (E.coli) bacteria with a chromosome which is not a linear polymer, but has a ring topology [3]. The biopolymers of DNA of some viruses such as bacteriophages λ that infect bacteria oscillate between linear and ring topology [4, 5]. The physical effects arising from confinement and chain topology play a significant role in the shaping of individual chromosomes and in the process of their segregation, especially in the case of elongated bacterial cells [6]. The behaviour of linear ideal and real polymers with excluded volume interaction (EVI) in a good solvent confined in a slit of two parallel repulsive [7, 8], inert or mixed walls is well understood [8]. Unfortunately, the physics of confined ideal ring polymers and ring polymers with EVI effects is still unclear. Ring polymers with specified knot type were chemically synthesized a long time ago [9]. Ring topology of polymers influences the statistical mechanical properties of these polymers, for example the scaling properties [10, 11] and shape [2, 12, 13] because it restrains the accessible phase space. An interesting point which was confirmed by numerical studies in [14] is that longer ring polymers are usually knotted with higher frequency and complexity. In [15], it was established that ring polymers with more complex knots are more compact and have a smaller radius of gyration and this decreases their ability to spread out under confinement. The results of Monte Carlo simulations performed in [16] suggest that the knotted ring polymers will exert higher entropic forces on the walls of the confining slit than the unknotted or linear polymers. In [16] it was stated that the knotted ring polymers expanded as the width of the slit increased in contrast to the behaviour of unknotted (or linear) polymers whose size showed a plateau after a certain width of slit was reached. The entropic force exerted on the walls arising from confinement to a slit of a knotted ring polymer was calculated using a bead-spring model by Matthews et al. in [5]. It was found [5] that in the case of a narrow slit, more complex knot types in a ring polymer exert higher forces on the confining walls of the slit in comparison to unknotted polymers of the same length, and for the relatively wide slits, the opposite situation takes

place. Confining ring polymer to a slab results in a loss of configurational entropy and leads to the appearance of a repulsive force which depends on the entanglements between two walls of the confining slab, as it was shown in the framework of a new numerical approach based on the generalized atmospheric sampling (GAS) algorithm for lattice knots in [17]. Thus, at the moment most of the papers devoted to the investigation of the behaviour of ring polymers compressed in confined geometries like slit or squeezed by a force in a slab of two parallel walls deal with numerical methods and present analytical results are incomplete. The above mentioned arguments stimulate us to apply one of the powerful analytical methods referred to as the massive field theory approach in a fixed space dimensions $d < 4$ (see [18, 19]) for the investigation of ring polymers confined to a slit geometry of two parallel walls or immersed in a solution of big mesoscopic colloidal particles of different size. This method, as it was shown in the series of papers [8, 20, 21], provides a good agreement with the experimental data and with the results of Monte Carlo simulations. We consider a dilute polymer solution, where different polymers do not overlap and the behaviour of such polymer solution can be described by a single polymer. As it is known, taking into account the polymer-magnet analogy developed by de Gennes [22, 23], the scaling properties of long-flexible polymers in the limit of an infinite number of steps N may be derived from a formal $n \rightarrow 0$ limit of the field theoretical ϕ^4 $O(n)$ -vector model at its critical point. In this case, the $1/N$ value plays the role of a critical parameter analogous to the reduced critical temperature in magnetic systems. Besides, we assume that the surfaces of the confining slit are impenetrable. It means that the correspondent potential $U(\tilde{z})$ of the interaction between the monomers of a polymer chain and a wall tends to infinity $U(\tilde{z}) \rightarrow \infty$ when the distance \tilde{z} between a wall and polymer is less than monomer size l . The deviation from the adsorption threshold [$c \propto (T - T_a)/T_a$] (where T_a is adsorption temperature) changes the sign at the transition between the adsorbed (the so-called normal transition, $c < 0$) and the nonadsorbed state (ordinary transition, $c > 0$) [24, 25] and it plays the role of a second critical parameter. The value c corresponds to the adsorption energy divided by $k_B T$ (or the surface enhancement in field theoretical treatment). The adsorption threshold for long-flexible polymers takes place, where $1/N \rightarrow 0$ and $c \rightarrow 0$. As was mentioned by de Gennes [22, 23], the partition function $Z(\tilde{\mathbf{x}}, \tilde{\mathbf{x}}')$ of a single polymer with two ends fixed at $\tilde{\mathbf{x}}$ and $\tilde{\mathbf{x}}'$ is connected with the two-point correlation function $G^{(2)}(\tilde{\mathbf{x}}, \tilde{\mathbf{x}}') = \langle \tilde{\phi}(\tilde{\mathbf{x}})\tilde{\phi}(\tilde{\mathbf{x}}') \rangle$ in ϕ^4 $O(n)$ -vector model for field $\tilde{\phi}(\tilde{\mathbf{x}})$ with the components $\phi_i(\tilde{x})$, $i = 1, \dots, n$ [and $\tilde{\mathbf{x}} = (\tilde{\mathbf{r}}, \tilde{z})$] via the $\mu_0^2 \rightarrow L_0$ inverse Laplace transform: $Z(\tilde{\mathbf{x}}, \tilde{\mathbf{x}}'; N, \nu_0) = \mathcal{I} \mathcal{L}_{\mu_0^2 \rightarrow L_0} (\langle \tilde{\phi}(\tilde{\mathbf{x}})\tilde{\phi}(\tilde{\mathbf{x}}') \rangle)_{n \rightarrow 0}$ in the limit, where the number n of components tends to zero. The conjugate Laplace variable L_0 has the dimension of length squared and is proportional to the total number of monomers N which form the polymer. The effective Ginzburg-Landau-Wilson Hamiltonian describing the system in semi-infinite ($i = 1$) or confined geometry of two parallel walls ($i = 1, 2$) is [24]:

$$\mathcal{H}[\tilde{\phi}, \mu_0] = \int d^d \tilde{x} \left[\frac{1}{2} (\nabla \tilde{\phi})^2 + \frac{\mu_0^2}{2} \tilde{\phi}^2 + \frac{\nu_0}{4!} (\tilde{\phi}^2)^2 \right] + \sum_{i=1}^2 \frac{c_{i_0}}{2} \int d^{d-1} \tilde{r} \tilde{\phi}^2, \quad (1)$$

where the conjugate chemical potential μ_0 is the “bare mass” in field-theoretical treatment, ν_0 is the “bare coupling constant” which characterizes the strength of EVI. In the case of slit geometry, the walls are located at the distance L one from another in \tilde{z} -direction in such way that the surface of the bottom wall is located at $\tilde{z} = 0$ and the surface of the upper wall is located at $\tilde{z} = L$. Each of the two surfaces is characterized by a certain surface enhancement c_{i_0} , where $i = 1, 2$. In the case when the ends of polymer $\tilde{\mathbf{x}}$ and $\tilde{\mathbf{x}}'$ in partition function $Z(\tilde{\mathbf{x}}, \tilde{\mathbf{x}}'; N, \nu_0)$ coincide, such partition function corresponds to the partition function of a phantom ring polymer, i.e., a ring polymer where we perform the summation over all possible knot structures. The fundamental two-point correlation function of the Gaussian theory corresponding to the effective Ginzburg-Landau-Wilson Hamiltonian (1) in a mixed $\tilde{\mathbf{p}}, \tilde{z}$ representation is: $G_{ij}^{(2)}(\tilde{\mathbf{p}}, \tilde{\mathbf{p}}'; \tilde{z}, \tilde{z}') = (2\pi)^{d-1} \delta_{ij} \delta(\tilde{\mathbf{p}} + \tilde{\mathbf{p}}') \tilde{G}_{\parallel}(\tilde{\mathbf{p}}; \tilde{z}, \tilde{z}'; \mu_0, c_{1_0}, c_{2_0}, L)$, where the free propagator $\tilde{G}_{\parallel}(\tilde{\mathbf{p}}; \tilde{z}, \tilde{z}'; \mu_0, c_{1_0}, c_{2_0}, L)$ of the model (1) in the case of ring polymer with coinciding ends $\tilde{\mathbf{x}} = \tilde{\mathbf{x}}' = \mathbf{x}$ can be obtained by analogy as it was done in [8] for linear polymer. It should be taken into account that we have ring polymer of length L_0 in a slit geometry of two parallel walls with fixed position of one monomer at point $\mathbf{x} = (\mathbf{r}, z)$ by analogy as it was proposed in [25] for description of ring polymer adsorption. Such representation assumes that the respective correlation function for ring polymer depends on $\mathbf{x} = (\mathbf{r}, z)$, e.g., on the position of some monomer which can be the first and the last monomer in the ring. Here, $\tilde{\mathbf{p}}, \tilde{\mathbf{p}}'$ are the values of parallel momentum associated with $d - 1$ translationally invariant directions in the system. The interaction between the polymer and the walls is implemented by the Dirichlet-Dirichlet

boundary conditions (D-D b.c.) (see [7, 8, 24]): $c_1 \rightarrow +\infty$, $c_2 \rightarrow +\infty$ or $\vec{\phi}(\mathbf{r}, 0) = \vec{\phi}(\mathbf{r}, L) = 0$. We consider the dilute solution of phantom ideal ring polymers and ring polymers with EVI immersed in a slit geometry of two parallel repulsive walls and permit the exchange of polymer coils between the slit and the reservoir. The polymer solution in the slit is in equilibrium contact with an equivalent solution in the reservoir outside of the slit. We follow the thermodynamic description of the problem as it was given in [7, 8] and perform the calculation in the framework of the grand canonical ensemble where the chemical potential μ is fixed. As it was shown in [7], the free energy of interaction between the walls in such a grand canonical ensemble is defined as the difference of the free energy of an ensemble where the separation of the walls is fixed at a finite distance L and where the walls are separated infinitely far from each other: $\delta F^R = -k_B T \mathcal{N} \ln \{ \mathcal{Z}_{\parallel}^R(L) / [\mathcal{Z}_{\parallel}^R(L \rightarrow \infty)] \}$, where \mathcal{N} is the total number of polymer coils in the solution and T is the temperature. The $\mathcal{Z}_{\parallel}^R(L)$ value is the partition function of one ring polymer located in a volume V containing two walls at a distance L . The correspondent *reduced free energy of interaction* δf per unit area $A = 1$ for the case of ring polymer confined in a slit geometry of two parallel walls after performing Fourier transform in the direction parallel to the surfaces and integration over $d^{d-1}r$ (which gives us the delta function $\delta(\mathbf{p})$ and leads to $\mathbf{p} = 0$ in the respective correlation functions after integration over $d^{d-1}p$) may be written in the form (see [8]):

$$\delta f^R = \frac{\delta F^R}{n_p k_B T} = L - \int_0^L dz \frac{\hat{\mathcal{Z}}_1^R(z)}{\hat{\mathcal{Z}}_b} + \int_0^\infty dz \left[\frac{\hat{\mathcal{Z}}_{HS_1}^R(z)}{\hat{\mathcal{Z}}_b} - 1 \right] + \int_0^\infty dz \left[\frac{\hat{\mathcal{Z}}_{HS_2}^R(z)}{\hat{\mathcal{Z}}_b} - 1 \right]. \quad (2)$$

Here, $n_p = \mathcal{N}/V$ is the polymer density in the bulk solution, and $\hat{\mathcal{Z}}_b = \mathcal{I} \mathcal{L}_{\mu_0^2 \rightarrow R_x^2/2}(\frac{1}{2\mu_0})$. The functions $\hat{\mathcal{Z}}_1^R(z)$ and $\hat{\mathcal{Z}}_{HS_i}^R(z)$ are equal to:

$$\hat{\mathcal{Z}}_1^R(z) = \mathcal{I} \mathcal{L}_{\mu_0^2 \rightarrow L_0} G^{(2)}(\mathbf{p} = 0; z, z) \Big|_{n \rightarrow 0}, \quad \text{and} \quad \hat{\mathcal{Z}}_{HS_i}^R(z) = \mathcal{I} \mathcal{L}_{\mu_0^2 \rightarrow L_0} G_{HS_i}^{(2)}(\mathbf{p} = 0; z, z) \Big|_{n \rightarrow 0},$$

where $G^{(2)}(\mathbf{p} = 0; z, z)$ and $G_{HS_i}^{(2)}(\mathbf{p} = 0; z, z)$ with $i = 1, 2$ are correlation functions of the model equation (1) describing the system in a slit geometry of two parallel walls and in semi-infinite geometry, respectively (see [8, 20]). Dividing the *reduced free energy of interaction* δf^R by another relevant length scale, for example, the size of the polymer in bulk, e.g. R_x (where $R_g^2 = \chi_d^2 R_x^2/2$, and χ_d is a universal numerical prefactor depending on the dimension d of the system (see [25],[26]) and R_g is the radius of gyration), yields the universal scaling function for the *depletion interaction potential* $\Theta^R(y) = \delta f^R/R_x$, where $y = L/R_x$. The resulting scaling function for the *depletion force* between the two walls induced by the polymer solution is denoted as (see [8]):

$$\Gamma^R(y) = -\frac{d(\delta f^R)}{dL} = -\frac{d\Theta^R(y)}{dy}. \quad (3)$$

As it is known [25], the resulting force exerted on the surfaces of a confining slit by polymer is equal to the resulting *depletion force* with the opposite sign: $K^R = d(\delta f^R)/dL$.

Let us consider at the beginning the case of phantom ideal ring polymer under Θ -solvent condition trapped in the slit geometry of two parallel repulsive walls. Taking into account that in the case of wide slit region we have $y \gtrsim 1$ for the scaling function of the *depletion force* Γ^R we obtain:

$$\Gamma_{DD}^{R,id}(y) = 2e^{-2y^2} - 8y^2 e^{-2y^2}. \quad (4)$$

The asymptotic solution for the *depletion force* in the narrow slit region, where $y \ll 1$, simply becomes: $\Gamma_{DD,narr}^{R,id} \approx -1$. The obtained results for the *depletion force* $\Gamma_{DD}^{R,id}$ are presented in figure 1 (a) by blue lines with triangles for a wide slit region and by green lines with triangles for a narrow slit region, respectively. It should be mentioned that the quantity Γ is normalized to the overall polymer density n_p . Thus, the above result simply indicates that the force is entirely induced by free chains surrounding the slit, or, in other words, by the full bulk osmotic pressure from the outside of the slit. We can state that in the case of very narrow slit with two repulsive walls, the ring polymers would pay a very high entropy to stay in the slit or even enter it. As the next step, let us consider the dilute solution of ring polymers with EVI in a good solvent immersed in a slit geometry of two parallel repulsive walls. As it is known [22, 23], in a good solvent the effects of the EVI between monomers play a crucial role so that the polymer

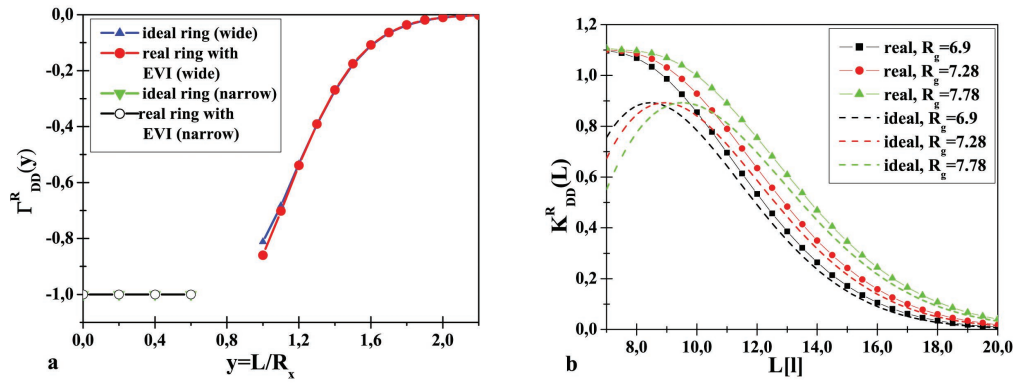


Figure 1. (Color online) (a) The scaling functions $\Gamma_{DD}^R(y)$ for phantom ideal ring and ring polymer with EVI in a good solvent immersed between two repulsive walls; (b) The functions $K^R(L)$ for phantom ideal ring polymer and ring polymer with EVI in a good solvent immersed between two repulsive walls for different values of the radius of gyration: $R_g(12_1) = 6.9 \pm 0.01[l]$ (black lines and black lines with squares); $R_g(9_1) = 7.28 \pm 0.01[l]$ (red dashed lines and red lines with dots); $R_g(6_1) = 7.78 \pm 0.01[l]$ (green dashed lines and green lines with triangles).

coils occupy a large space compared to the case of ideal polymers. The calculations of the correspondent partition functions $\hat{\mathcal{Z}}_1^R(z)$ and $\hat{\mathcal{Z}}_{HS_i}^R(z)$, which permit to obtain the reduced free energy of interaction δf^R in equation (2), are connected with the calculations of the correspondent correlation functions $G^{(2)}(\mathbf{p} = 0; z, z)$ and $G_{HS_i}^{(2)}(\mathbf{p} = 0; z, z)$ with $i = 1, 2$ where the terms describing the EVI effects are taken into account via using perturbation treatment in the framework of the massive field theory approach in a fixed space dimensions $d = 3$ up to one-loop order approximation. In order to make the theory UV finite in RG sense directly in $d = 3$ space dimensions, we perform a standard mass renormalization $\mu_0^2 = \mu^2 - \delta\mu_0^2$ and the coupling constant renormalization $\nu_0 = \mu\nu$ of the above mentioned correlation functions by analogy as it was proposed by Parisi [19]. Besides, the surface enhancement renormalization $c_{i_0} = c_i + \delta c_i$ of the correspondent correlation functions in the case of D-D b.c. reduces to an additive renormalization as it took place in the case of semi-infinite geometry [20] and slit geometry (see [8]). The correspondent expression for the scaling function of the *depletion force* between two repulsive walls in the case of wide slit region $y \gtrsim 1$ is:

$$\Gamma_{DD}^{R, \text{real}}(y) = 2e^{-2y^2} - 8y^2e^{-2y^2} - \frac{\bar{\nu}}{2}e^{-2y^2} \left[\frac{1}{y^2} + 2\sqrt{\pi}\psi^{(0)}\left(-\frac{1}{2}\right) - D - 4yB(y) \right], \quad (5)$$

where $D = \frac{1}{4} [10 - 2\ln 2 - 2\psi^{(0)}(-\frac{1}{2}) + \sqrt{\pi}\psi^{(0)}(\frac{1}{2}) - 2\gamma_E]$, $B(y) = [2y\sqrt{\pi}\psi^{(0)}(-\frac{1}{2}) - \frac{1}{y}]$ and $\gamma_E = 0.577$ is the Euler's constant, $\psi^{(0)}(z)$ is the digamma function, $\text{erfc}(z) = 1 - \text{erf}(z)$ is the complementary error function. Besides, the $\nu = b_n \bar{\nu}$ value was introduced with $b_n = \frac{6}{n+8} \frac{(4\pi)^{3/2}}{\Gamma(1/2)}$ and the calculations are performed at the correspondent fixed point $\bar{\nu}^* = 1$ in the limit $n \rightarrow 0$. In the region of a very narrow slit $y \ll 1$ the *depletion force* is: $\Gamma_{DD, \text{narr}}^{R, \text{real}} \approx -1$. The results of calculations for $\Gamma_{DD}^{R, \text{real}}$ are presented in figure 1 (a) by the red line with circles in a wide slit region and by the black line with open circles in a narrow slit region, respectively. As it is easy to see from figure 1 (a), the obtained results for the scaling function for the *depletion force* in the case of ring polymer immersed between two repulsive walls are characterized by a completely different behaviour compared to the case of linear polymer (see [8]). The phantom ring polymer, due to the complexity of chain topology and for entropical reasons, tends to escape from the space between two repulsive walls and it leads to the attractive *depletion force* between the confining walls. Besides, we observe [see figure 1 (a)] that the absolute value of the scaling function for the *depletion force* for phantom ring polymers in the wide slit region is smaller than for linear polymer chains (see [8]) and decreases as the width of the slit increases. In figure 1 (b) we present the results for the entropically induced force K^R (as functions of L for different values of radius of gyration R_g) which exerts phantom ideal ring polymer and ring polymer with EVI on the confining two repulsive walls. It should be mentioned that calculations, presented in figure 1 (b) were performed for different values of radius of

gyration [5]: $R_g(12_1) = 6.9 \pm 0.01[l]$, $R_g(9_1) = 7.28 \pm 0.01[l]$, and $R_g(6_1) = 7.78 \pm 0.01[l]$ which correspond to the ring polymers with different knot types: $12_1; 9_1; 6_1$. Here, C_p is a standard notation [27], where C denotes the minimum number of crossings in any projection on a plane and p is used in order to distinguish the knot types with the same C . It should be mentioned that the region of validity of the obtained results for the entropically induced forces K^R for phantom ideal ring polymers [see figure 1 (b)] is defined by the value of $y = L/R_x \gtrsim 1$ with $R_x = \sqrt{2}R_g$. We observed that in the wide slit region, ring polymers with less complex knot types (with bigger radius of gyration) in a ring topology exert higher forces on the confining walls [see figure 1 (b)] at the same length L . In figure 2 (a), we present the ratio $K_{DD}^R/K_{DD}^{\text{lin}}$ of force for ring polymer chains and corresponding force for linear polymer chains in a slit geometry of two parallel repulsive walls as function of the distance L between the walls for different values of the radius of gyration R_g . Our results for entropically induced force K^R are in agreement with the previous results obtained by Matthews et al. in [5] using a bead-spring model. The difference between our results and the results obtained by Matthews et al. arises due to the fact that in [5] calculations were performed for relatively short polymer chains with polymer length of order $N \sim 300$ units. Taking into account the Derjaguin approximation [28], which describes the sphere of the big colloidal particle by a superposition of immersed plates with local distance from the wall (or from other particle), we performed calculations of the depletion force $-d[\Phi_{DD}^R(\tilde{y})/(n_p k_B T)]/d\tilde{y}$ between colloidal particle and a wall (or between two colloidal particles) in a dilute solution of ring polymers. It should be mentioned that $\Phi_{DD}^R(\tilde{y})/(n_p k_B T)$ is equal to $2\pi\tilde{R}R_x^2 \int_{\tilde{y}}^{\infty} dy \Theta^R(y)$ with $\tilde{y} = a/\sqrt{2}R_g$ (where a is the minimal distance between the sphere and the wall) and $\tilde{R} = R$ for the case of big colloidal particle of radius $R \gg L$ (and $R \gg R_g$) near the wall and $\tilde{R} = R_1 R_2 / (R_1 + R_2)$ for the case of two colloidal particles with different radius $R_1 \neq R_2$ (when $R_i \gg L$ and $R_i \gg R_g$, $i = 1, 2$). The results of calculations are presented in figure 2 (b) and indicate that the absolute value of the depletion force which arises between two colloidal particles is smaller than between particle and wall. Besides, if the number of coils \mathcal{N} can be fixed, then the total free energy of the polymer solution within the slit in the canonical ensemble can be obtained from our results for the grand canonical free energy via the Legendre transform by analogy as it took place in [7, 8] for linear polymers. The further investigation of solution of ring polymers with EVI immersed in a slit geometry of two inert walls or mixed walls as well as the investigation of polymer-colloid interactions for different sorts of colloids is the task of great interest which is under consideration.

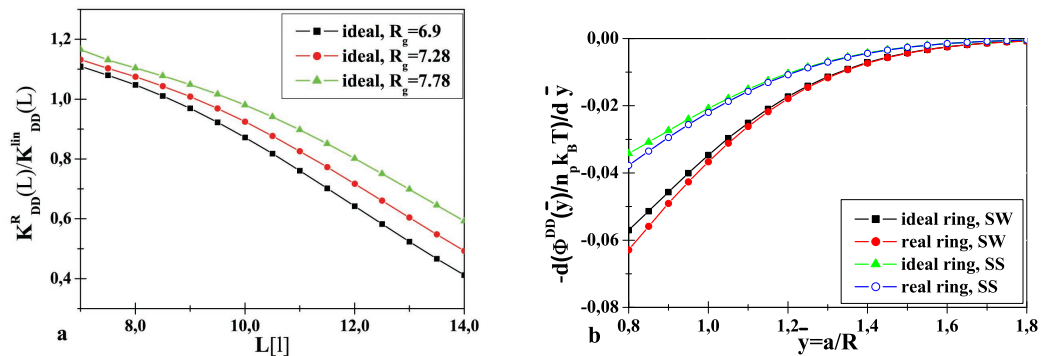


Figure 2. (Color online) (a) The ratio $K^R(L)/K^{\text{lin}}(L)$ as function of the distance L (in l units) between the walls for different values of R_g ; (b) The functions $-d[\Phi_{DD}^R(\tilde{y})/(n_p k_B T)]/d\tilde{y}$ for phantom ideal ring polymer and ring polymer with EVI in a good solvent immersed between colloidal particle and wall as well as between two colloidal particles.

References

1. Marek J., Demjénová E., Tomori Z., Janáček J., Zolotová I., Valle F., Favre M., Dietler G., *Cytometry, Part A*, 2005, **63A**, 87; doi:10.1002/cyto.a.20105.
2. Witz G., Rechendorff K., Adamcik J., Dietler G., *Phys. Rev. Lett.*, 2011, **106**, 248301; doi:10.1103/PhysRevLett.106.248301.

3. Berg J., Tymoczko J., Stryer L., Biochemistry, 5th Ed., Freeman W.H. and Co., New York, 2002.
4. Arsuaga J., Vazquez M., Trigueros S., Sumners D.W., Roca J., Proc. Natl. Acad. Sci. U.S.A., 2002, **99**, 5373; doi:10.1073/pnas.032095099.
5. Matthews R., Louis A.A., Yeomans J.M., Mol. Phys., 2011, **109**, 1289; doi:10.1080/00268976.2011.556094.
6. Jun S., Mulder B., Proc. Natl. Acad. Sci. U.S.A., 2006, **103**, 12388; doi:10.1073/pnas.0605305103.
7. Schlesener F., Hanke A., Klimpel R., Dietrich S., Phys. Rev. E, 2001, **63**, 041803; doi:10.1103/PhysRevE.63.041803.
8. Romeis D., Usatenko Z., Phys. Rev. E, 2009, **80**, 041802; doi:10.1103/PhysRevE.80.041802.
9. Dietrich-Buchecker C.O., Sauvage J.P., Angew. Chem. Int. Ed., 1989, **28**, 189; doi:10.1002/anie.198901891.
10. Dobay A., Dubochet J., Millett K., Sottas P.-E., Stasiak A., Proc. Natl. Acad. Sci. U.S.A., 2003, **100**, 5611; doi:10.1073/pnas.0330884100.
11. Ercolini E., Valle F., Adamcik J., Witz G., Metzler R., De Los Rios P., Roca J., Dietler G., Phys. Rev. Lett., 2007, **98**, 058102; doi:10.1103/PhysRevLett.98.058102.
12. Alim K., Frey E., Phys. Rev. Lett., 2007, **99**, 198102; doi:10.1103/PhysRevLett.99.198102.
13. Rawdon E.J., Kern J.C., Piatek M., Plunkett P., Stasiak A., Millett K.C., Macromolecules, 2008, **41**, 8281; doi:10.1021/ma801389c.
14. Janse van Rensburg E.J., Whittington S.G., J. Phys. A: Math. Gen., 1990, **23**, 3573; doi:10.1088/0305-4470/23/15/028.
15. Quake S., Phys. Rev. Lett., 1994, **73**, 3317; doi:10.1103/PhysRevLett.73.3317.
16. Janse van Rensburg E.J., J. Stat. Mech.: Theory Exp., 2007, **2007**, P03001; doi:10.1088/1742-5468/2007/03/P03001.
17. Gasumova D., Janse van Rensburg E.J., Rechnitzer A., J. Stat. Mech.: Theory Exp., 2012, **2012**, P09004; doi:10.1088/1742-5468/2012/09/P09004.
18. Parisi G., J. Stat. Phys., 1980, **23**, 49; doi:10.1007/BF01014429.
19. Parisi G., Statistical Field Theory, Addison-Wesley, Redwood City, 1988.
20. Diehl H.W., Shpot M., Nucl. Phys. B, 1998, **528**, 595; doi:10.1016/S0550-3213(98)00489-1.
21. Usatenko Z., J. Chem. Phys., 2011, **134**, 024119; doi:10.1063/1.3529426.
22. De Gennes P.G., Phys. Lett. A, 1972, **38**, 339; doi:10.1016/0375-9601(72)90149-1.
23. De Gennes P.G., Scaling Concepts in Polymer Physics, Ithaca: Cornell University Press, New York, 1979.
24. Diehl H.W., In: Phase Transitions and Critical Phenomena Vol. 10, Domb C., Lebowitz J.L. (Eds.), Academic Press, London, 1986, 75–267.
25. Eisenriegler E., Polymers Near Surfaces, World Scientific, Singapore, 1993.
26. Des Cloizeaux J., Jannink G., Polymers in Solution, Clarendon Press, Oxford, 1990.
27. Orlandini E., Whittington S., Rev. Mod. Phys., 2007, **79**, 611; doi:10.1103/RevModPhys.79.611.
28. Derjaguin B.V., Kolloid Z., 1934, **69**, 155; doi:10.1007/BF01433225.

Кільцеві полімери в обмежених середовищах

З. Усатенко¹, Й. Халюн², П. Кутерба²

¹ Інститут Фізики, Краківський Політехнічний Університет, 30-084 Краків, Польща

² Інститут Фізики, Ягеллонський Університет, 30-348 Краків, Польща

Проведено дослідження розведених розчинів ідеальних кільцевих та кільцевих полімерів з ефектами виключеного об'єму в доброму розчиннику, обмежених в щілині двох паралельних відштовхуючих поверхонь, а також у розчині колоїдних частинок великого розміру. Беручи до уваги відповідність між теретикопольовою ϕ^4 $O(n)$ -векторною моделлю в границі $n \rightarrow 0$ і поведінкою довгих гнучких полімерів в доброму розчиннику, було отримано з використанням масивної теорії поля при фіксованій вимірності простору $d = 3$ в рамках однопетлевого наближення відповідні сили збіднення і сили, які діють між ідеальними кільцевими та кільцевими полімерами з ефектами виключеного об'єму і стінками щілини. Окрім того, беручи до уваги наближення Дерягіна, розраховано сили збіднення між колоїдною частинкою і стінкою, а також між двома колоїдними частинками великого розміру. Отримані результати вказують на те, що кільцеві полімери через складність топології і з ентропійних причин демонструють цілком іншу поведінку в обмежених середовищах ніж лінійні полімери.

Ключові слова: колоїдні системи, критичні явища, полімери, фазові переходи